Large effect life-history genomic regions are associated with functional morphological traits in Atlantic salmon

Tutku Aykanat[1], Paul V. Debes[2,6], Shadi Jansouz[1], Lison Gueguen[3], Jaakko Erkinaro[4], Victoria L. Pritchard[5], Craig R. Primmer[1,6], Geir H. Bolstad[7]

1. Organismal and Evolutionary Biology Research Program, Faculty of Biological and Environmental Sciences, PO Box 56, FI-00014 University of Helsinki, Finland. tutku.aykanat@helsinki.fi.
2. Department of Aquaculture and Fish Biology, Hólar University, 550 Sauðárkrókur, Iceland.
3. Oniris Graduate School of Veterinary Medicine, Nantes, France.
4. Natural Resources Institute Finland (Luke), Oulu, Finland
5. Institute for Biodiversity & Freshwater Conservation, UHI Inverness, Inverness, United Kingdom.
6. Institute of Biotechnology, Helsinki Institute of Life Science (HiLIFE), University of Helsinki, Helsinki, Finland.
7. Norwegian Institute for Nature Research (NINA), NO-7485 Trondheim, Norway.

Abstract

Understanding pleiotropic architectures of phenotypes is instrumental for identifying the functional basis of adaptive genetic variation in the wild. Life-history variation may have a morphological basis that mediates resource acquisition and allocation pathways, but identifying the underlying genetic basis of such traits is challenging. In this study, using Atlantic salmon juveniles reared in common garden conditions, we test if two life-history associated loci in Atlantic salmon, s*ix6* and *vgll3,* are also associated with functional morphological traits. These loci had previously shown to exhibit strong signals of adaptation and are highly correlated with age at maturity. Here, we show that genetic variation at the *vgll3* locus is linked to variation in morphological traits that underlie swimming performance, along a trade-off axis between efficient cruising and maneuvering, while the genetic variation at the *six6* locus was linked to variation in body-head proportions suggesting the potential functional importance of these traits for resource acquisition efficiency. However, the direction of changes in morphological traits associated with late- vs. early- maturing alleles was not always consistent with the expected direction of an effect to maturation timing. Our results reveal a complex morphological landscape associated with the genetic variation in these loci, possibly as a result of pleiotropy or linkage across these genomic regions.

Keywords: Atlantic salmon, morphology, morphometrics, adaptive genetic variation, age at maturity, pleiotropy, *six6*, *vgll3*

Introduction

Elucidating the genotype-phenotype relationship is instrumental to identifying the functional basis of adaptation, and the potential targets of selection (Barrett and Hoekstra, 2011; Kawecki and Ebert, 2004; Nielsen *et al*, 2009; Wagner and Altenberg, 1996). Methodological and statistical advances in genetics now allow the identification of genomic regions responding to local selection, but the phenotypic link between genotype and fitness is often missing. Furthermore, many genomic regions can affect a multitude of phenotypic traits (via pleiotropy or linkage disequilibrium), which makes identifying the phenotypic traits under selection even more challenging (Paaby and Rockman, 2013; Solovieff *et al*, 2013). Even large-genome-wide association studies might be underpowered to detect pleiotropy (Wagner and Zhang, 2011), a methodological bias by which the adaptive significance of pleiotropy can be overlooked especially in natural, non-model populations even if it may have substantial effects to limit, or promote adaptation (Orr, 2000; Otto, 2004). In natural systems, pleiotropy has been mostly studied at the phenotypic level to understand the evolutionary trade-offs by quantifying the physiological antagonisms between the senescence and reproduction age. Yet, some studies identify pleiotropic effects of genes associated with adaptive genetic variation. For example, adaptive divergence between lake vs. marine morphs of threespine stickleback (*Gasterosteus aculeatus*) was explained by both pleiotropy in the *Eda* gene, and via strong linkage with the surrounding loci (Archambeault *et al*, 2020), illustrating the significance of such genetic architectures for adaptation.

Genomic regions with large adaptive importance are more likely to be detected in genome scans for selection and are likely to have broad cellular and phenotypic effects (Chan *et al*, 2010; Colosimo *et al*, 2005). Major effect loci may have roles at critical nodes of the regulatory networks, which have high centrality and connectivity, and could thereby drive strong genetic interdependences among traits (Chan *et al*, 2010; Colosimo *et al*, 2005; Jimenez-Gomez *et al*, 2010; Weith *et al*, 2023) but see (Boyle *et al*, 2017; Jakobson and Jarosz, 2020). Therefore, loci exhibiting strong signals of adaptation may provide feasible empirical approaches to understand the significance of complex evolutionary processes, such as how pleiotropy and genetic interactions may hinder or promote adaptation in relation to the direction of natural selection between co-varying traits. Yet, such examples remain rare in non-model, wild organisms (Archambeault *et al*, 2020; Endler, 2000; Mackay *et al*, 2009; Olson-Manning *et al*, 2012).

Functional variation in morphological traits is integral in shaping resource use, and is correspondingly associated with life-history variation and ecotypic divergence in a large array of fish species, including salmonid fishes (Ferry-Graham *et al*, 2002; Fitzgerald *et al*, 2017; Keeley *et al*, 2005; Lundsgaard-Hansen *et al*, 2013; Mindel *et al*, 2016; Proulx and Magnan, 2004; Svanbäck and Eklöv, 2003; Taylor and McPhail, 1985; Varian and

Nichols, 2010; Webb, 1988). For example, a fusiform body and shorter fins appear adaptive to a long-distance migratory strategy, likely because this body shape reduces the drag (hence the energy consumed) during migration (Morinville and Rasmussen, 2007). Likewise, a robust body shape with larger head, caudal peduncle, and paired fins has been associated with piscivory in rainbow trout (*Oncorhynchus mykiss*, Keeley *et al*, 2005). Recent population genomics studies in Atlantic salmon have consistently identified two unlinked genomic regions, surrounding the genes *six6* in chromosome 9 and *vgll3* in chromosome 25 as strong targets for local selection within all European Atlantic salmon lineages (Barson *et al*, 2015; Miettinen *et al*, 2023; Pritchard *et al*, 2018; Zueva *et al*, 2020). These two loci have also been linked to a suite of life-history traits that strongly influence fitness. In particular, the *vgll3* and *six6* loci are strongly associated with age-at-first-maturity in seagoing salmon at the individual- and population- levels respectively (Barson *et al*, 2015) (see also, Ayllon *et al*, 2015; Sinclair-Waters *et al*, 2020), and the *vgll3* locus affects other alternative life-history strategies, such as precocious male maturation (Debes *et al*, 2021), and iteroparity (Aykanat *et al*, 2019). Similarly, these loci explain variation across a number of metabolic and behavior traits: *vgll3* has been shown to be associated with aggression, maximum metabolic rate, and aerobic scope at the juvenile stage (Bangura *et al*, 2022; Prokkola *et al*, 2022), while *six6* predicts diet acquisition at sea in maturing adults migrating towards fresh waters (Aykanat *et al*, 2020), and exhibits epistasis with *vgll*3 to effect aerobic scope variation (Prokkola *et al*, 2022). The strong genetic interdependence of these phenotypic traits across two loci points to the potential for a shared developmental origin (of phenotypes to the respective loci), which is supported by the role of *vgll3* and *six6* in the hormonal and cell-fate commitment gene-expression pathways (Ahi *et al*, 2022; Kurko *et al*, 2020; Verta *et al*, 2020; Verta *et al*, 2024) and broad expression of *six6* during early development (Moustakas-Verho *et al*, 2020). Finally, a recent study showed both loci are linked to early life survival in juvenile Atlantic salmon, albeit via parental genetic effects, further supporting broad functional roles across life stages (Aykanat *et al*, 2024). This collective evidence indicates that these loci are broad-scale modulators of salmon phenotype, yet their effect on morphological variation, if any, is not known.

In order to characterize the morphological variation associated with these locally adaptive genomic regions, in this study, we quantified morphometric variation in more than 700 juvenile Atlantic salmon reared in common garden conditions and related it to *six6* and *vgll3* genotype using a mixed modelling approach that also controls for confounding effects of length and condition factor. We identified a suite of morphological characters correlated to the variation in the *vgll3* and *six6* loci. Our study extends the broad pleiotropic effect of *vgll3* and *six6* loci to functional morphological traits, including phenotypes that are likely important targets of natural selection.

Materials and Methods

Fish breeding and rearing and common garden conditions

Details of breeding and rearing of individuals from the same cohort were provided in Debes *et al* (2021), using a similar experimental procedure and facilities, except that fish in the present study were reared in approximately 2° C cooler water temperature (See, Debes *et al* 2019, for the details of the rearing temperature). Briefly, the parents of the individuals used were 44 Baltic lineage Atlantic salmon from a broodstock maintained by the Natural Resources Institute Finland (Laukaa, Finland) that were initially originated from the Neva River in Russia (Gulf of Finland in the Eastern Baltic Sea) and has been used for juvenile salmon supplementation in the Kymi river in South-Eastern Finland (Asheim *et al*, 2023). Parents were crossed to have balanced representation of homozygote genotypes in the *vgll3* locus between early (E) and late (L) maturing alleles (i.e. $vgll3^{EE}$ and $vgll3^{LL}$, Supplementary Table 1). *Six6* genotype distribution was not considered during the breeding design, but was nevertheless segregating in a number of families (Supplementary Table 1). Crosses were performed in November 2017 and offspring reared in the University of Helsinki fish facilities, first in replicated family-specific compartments in vertical incubators until the swim-up stage, and then subsequently offspring of all families were mixed in eight tanks with roughly balanced proportions of families per tank (Supplementary Table 2). The rearing temperature of fish in this study followed a seasonal cycle (range: 4.1– 16.0°C) and the natural light regime of the latitude (61.054° N) as described in Debes *et al* (2019). In August 2018, the fish were individually PIT-tagged and a fin clip sample was taken to identify the families via genetic pedigree reconstruction. Fish were fed ad libitum except for a short period of restricted feeding for half of the tanks, which included ad libitum feeding for two days and then no feeding for five days, each week for a five week period (Debes *et al*, 2021).

Landmarking and trait measurements

Morphological data were collected as part of a larger effort in December 2018. Fish of both sexes were euthanized using an overdose of tricaine methanesulphonate bath, and stored for a short time on ice until imaging was performed the same day. Each fish was sliced ventrally to collect data on gonad development for another study. The fish was placed on graphical paper and the body image was taken using a digital camera (Canon PowerShot S110) mounted on a tripod (Hama Star 61), with aperture-priority exposure at F:8, and auto focus option (Supplementary Figure 1). Cross sections were obtained by slicing the fish at the posterior end of the dorsal fin (hereafter termed as large cross section) and adipose fins (hereafter termed as small cross section), respectively. These were placed on a transparent sheet and digitized using a scanner (Epson XP-305) with a modified lid to accommodate the depth of the cross sections (Supplementary Figure 1).

Landmarks were placed on the whole body and the two cross-sections at a randomized order using imglab software (Porto *et al*, 2020), by two of the co-authors (LG for landmarked body planes, and SC for landmarked cross sections) who were blind to any information related to the genotypes or sex of the fish (Supplementary Figure 2). Landmarks were not placed around the gut region due to the previous ventral slicing. Some landmarks were solely used in the Procrustes analysis to quantify shape, while others used to quantify specific trait values by calculating the distance between landmarks (Supplementary Figure 2, Table 1). Traits that were measured twice on both the left and right side (Table 1), were averaged prior to analysis. All measurements were reported in centimeters (cm).

Data Filtering

At the time of sampling, fish exhibited a bimodal length distribution which is often observed within juvenile salmon from the same cohort (Hoar, 1988). At the time of sampling a majority of fish used in the analysis (i.e. upper mode of size distribution, see below) had a complete smolt appearance (base on the disappearance of parr marks in the skin and silvery coloration, e.g., Debes *et al*, 2020), or were at late stages of smoltification (faint parr marks with close to silvery skin coloration). We excluded a small number of fish in the lower mode to avoid potential interactions associated with this size bimodality (fish fork length < 9 cm, N=69, Supplementary Figure 3). In addition, fish with missing *vgll3* and *six6* genotypes, and sex (N=2, N=12, and N=4, respectively), and a small number of precociously matured males (N=19) were excluded from the analysis. Missing landmarks (0.02 % of the total landmarks) were imputed using the *estimate.missing* function in the *geomorph* package (version 4.0.6, Baken *et al*, 2021). A landmarked image was excluded from the analysis if more than one landmark was identified as an outlier in the Procrustes analysis (i.e. > 4 sd away from the mean). These landmarks were not corrected manually, to avoid introducing among technician variation. After data filtering, 821 individuals remained in the dataset, of which 731, 737, and 772 individuals were in the small cross section, large cross section, and whole body datasets, respectively, (Supplementary Table 1). 16, 18, and 712 individuals were landmarked more than once to estimate repeatability. Landmarkinng for the first 30 and 50 images per researcher for body and cross sections, respectively, were discarded as training sets.

Trait measurements

We quantified variation in 21 traits across various body planes with potential functional significance using the landmark positions (Supplementary Figure2) and as formulated in Table 1.

<u>*Rayed fins and caudal peduncle length:*</u> We measured the length of dorsal, anal, and tail fins, between interior and exterior insertion points, as well as the caudal peduncle (Table 1, Supplementary Figure 2). The variation in these traits may be associated with habitat use, feeding, and swimming performance in salmonids, and other

155 fishes (e.g., Jonsson and Jonsson, 2011a; Keeley *et al*, 2005). Increased dorsal and pectoral fin sizes in fish are
156 likely important for increase maneuverability and stability, and likely important adaptations for faster flowing
157 streams (Webb, 1984). Specifically, large paired fins (such as pectoral and pelvic fins) in Atlantic salmon are
158 associated with populations that occupy faster flowing and colder streams than slower flowing and warmer
159 rivers, an adaptation attributed to providing effective stability under fast flowing, and turbulent currents
160 (Riddell and Leggett, 1981; Webb, 1988). In Coho salmon, juveniles of interior populations with longer
161 migration distances appear to have smaller fins (Taylor and McPhail, 1985), which may help to reduce drag in
162 long migrations (Varian and Nichols, 2010).

163 *Eye diameter and position, and snout length*: The size of the eye was approximated from the diameter, and the
164 snout length was measured as the distance between the center of the eye to the anterior extreme of the head
165 (Table 1, Supplementary Figure 2). These traits are morphological features associated with trophic
166 specialization and habitat use across fish taxa (Elmer *et al*, 2010; Peris Tamayo *et al*, 2020; Snorrason, 1994).

167 *Aerobic muscle:* We approximate the area of aerobic muscle fibers (also called slow-twitch muscle, or red
168 muscle) by measuring the landmark distances in the cross sections from the lateral line towards the transverse
169 sections, and by measuring the extent of the red muscle along the lateral line (Table 1, Supplementary Figure
170 2). Aerobic muscle provides energy required during steady, cruise swimming, and helps with thermal
171 acclimation in fishes (Altringham and Ellerby, 1999; Shuman and Coughlin, 2018). Recently, it has been shown
172 that both *vgll3* and *six6* loci are associated with whole body aerobic activity (Prokkola *et al*, 2022), which is a
173 critical physiological process in salmonid life cycle (Eliason and Farrell, 2015), which may indicate that aerobic
174 muscle mass, as a proxy for aerobic activity, may be associated with these loci.

175 *Cross sectional centroid size and diameter, and vertebral thickness*: We measured cross sectional centroid size
176 and horizontal diameter from both large and small cross-section images (Table 1, Supplementary Figure 2), as
177 approximation for fusiform body shape. A slimmer and more torpedo-shape provides improved energy
178 efficiency during cruising and in high flow streams via reducing the water drag, and it is an important life
179 history adaptation among fishes (Crossin *et al*, 2004; Jonsson and Jonsson, 2011a; Taylor and McPhail, 1985;
180 Webb, 1988). In contrast, a robust cross-section facilitates burst swimming, which is advantages for prey
181 avoidance, and food acquisition (Taylor and McPhail, 1985).

182 We also quantified vertebral width as a proxy for cone diameter, to approximate vertebra's flexibility/stiffness
183 during the lateral bending movement in the undulated motion, which help maintaining steady swimming at the
184 expense of maneuvering capabilities (Baxter *et al*, 2022; Donatelli *et al*, 2021; Long and Nipper, 1996).

185 *Head and body size:* We quantified head length and width (Table 1, Supplementary Figure 2), which are
186 important determinants of ecotypic divergence via resource and habitat use in fishes (Peris Tamayo *et al*, 2020;
187 Simonsen *et al*, 2017). A larger head and larger snout length may be associated with feeding regime towards
188 piscivory (Keeley *et al*, 2005), or generally speaking, consuming larger prey items. We also measured head and
189 body centroid sizes as an approximation for the area of the morphometric planes, which is the square root of
190 the sum of squared distances of all the landmarks used in the Procrustes analysis from the point of center of
191 gravity (Klingenberg, 2016). The Atlantic salmon has a smaller head-body ratio, compared to the brown trout
192 (Jonsson and Jonsson 2011), which likely makes salmon more efficient swimmers both in strong freshwater
193 currents and during longer marine migrations.

194 *Statistical analysis*

195 Our analysis framework comprised of a series of analyses whereby Procrustes shape variable, and
196 morphological traits were used as response variables. These analyses were conducted independently for body,
197 small cross section, and large cross section. In all analyses length (centered to zero and scaled to have a unit
198 standard deviation), body condition (Fulton's condition factor, scaled), sex, and food treatment were used as
199 covariates. In all models, we implemented genetic variation as additive, where *vgll3* and *six3* genetic effects are
200 coded as 0, 1, and 2 for EE, EL, and LL genotypes respectively (E and L refer to the alleles associated with early
201 and late maturation, respectively), so that a unit change in genetic effect represent an additive allelic
202 substitution effect from E to L. Unless otherwise noted, all statistical analysis were performed in R software
203 version 4.4.1 (R Core Team, 2019).

204 We performed multivariate generalized Procrustes analysis to quantify shape variation (Gower, 1975), using
205 the default settings in the *gpagen* function in the geomorph package (version 4.0.8, Baken *et al*, 2021). This
206 function outputs Procrustes shape variables, centered on the mean value for each landmark and normalized for
207 centroid size. Centroid size is the square root of the sum of squared distances of landmarks from the center of
208 gravity (i.e., centroid) and it is highly correlated to size of the fish.

209 Procrustes shape data was then used to perform a Procrustes linear regression analysis using the *procD.lm*
210 function with default settings (i.e. residual randomization was used for significance testing and type III marginal
211 sums of squares for cross products computations). The model parameters were as follows:

212 $Y = \mu + L + CF + Feed + Tank + Sex + Vgll3 + Six6 + Fam + \varepsilon_{error}$

213 Where Y is the multivariate data frame consisting of x and y coordinates for Procrustes shape coordinates of
214 landmarks, μ is the intercept, L is the scaled fork length, CF is the scaled Fulton's condition factor, and Feed is

215 the factor associated with feed treatment (ad-libitum vs restricted feed). Other terms are the rearing tank ID
216 that the fish were reared after the swim-up stage (Tank), sex (Sex), family (Fam), and the additive genetic
217 effects for *vgll3* and *six6*, respectively. Since, the *procD.lm* function does not accommodate random terms, we
218 included tank and family effects as fixed terms. Trait values were averaged prior to the analyses when an
219 individual had replicate measurements. We reported multivariate analysis of variance Pillai's trace statistics,
220 estimated using the *manova.update* function in the RRPP package (version 2.0.3, Collyer *et al*, 2018), and plot
221 individuals landmark differences between loci using the *plotRefToTarget* in the geomorph package.

222 To decompose the variation associated with trait values and estimate parameter coefficients, we employed a
223 linear mixed effect (animal) model using the *relmatLmer* function in lme4qtl (version 0.2.2, Ziyatdinov *et al*,
224 2018), which is an implementation of *lmer* function in lme4 package (Bates, 2010), and can fit the animal model
225 (i.e., accommodate the additive relatedness matrix). When estimating fixed coefficients, the model was fitted
226 with maximum likelihood using the *REML = FALSE* option in the *relmatLmer* function. The model structure was
227 as follows:

228 $Y = \mu + L + CF + Feed + Sex + Vgll3 + Six6 + \varepsilon_{ID} + \varepsilon_{tank} + \varepsilon_{animal} + \varepsilon_{error}$

229 Fixed effect terms are as described above except that the fixed tank and family terms in the previous model
230 were replaced with random tank and animal terms, respectively. Random terms thus included, ε_{ID} which are
231 the individual effects, ε_{tank} are the effects associated with the tank effects, and ε_{error} is the measurement error.
232 ε_{animal} is the random term associated with the background genetic effects after controlling for *vgll3* and *six6*
233 fixed effects. The relatedness matrix was obtained using the pedigree data in Debes *et al* (2019) using *getA*
234 function in the pedigreem package (version 0.3.4, Vazquez *et al*, 2010). Since we used repeated measurements
235 in the analysis, ε_{ID} reflects the error term, while ε_{error} are residuals that quantifies deviations between repeated
236 samples (i.e. measurement error).

237 The significance of the fixed effects terms was estimated using the *as_lmerModLmerTest* function in the
238 lmerTest package (version 1.1-3, Kuznetsova *et al*, 2017) in R using type 3 F test with Satterthwaite's method to
239 estimate the effective degrees of freedom.

240 We then estimated the additive genetic variation, the contribution of *vgll3* and *six6* loci to the additive genetic
241 variation, evolvability, and repeatability. For these, we employed three models similar to above, but the first
242 model ($Model_{VA.full}$) did not contain *vgll3* or *six6* to estimate total additive genetic variation, and was fitted
243 using the *REML = TRUE* option in the *relmatLmer* function to obtain unbiased estimates of variance
244 components. As such, variance of ε_{animal} (V_{animal}) in the $Model_{VA.full}$ is the total additive genetic variation (V_A).
245 Percent contribution of *vgll3* and *six6* are calculated as $\%V_{A.vgll3} = 100 * ((2 \times L_{vgll3} \times E_{vgll3} \times (\beta_{vgll3}^2 - se(\beta)_{vgll3}^2) /$

V_{animal}), and $\%V_{A.six6} = 100 * ((2 \times L_{six6} \times E_{six6} \times (\beta_{six6}^2 - se(\beta)_{six6}^2))) / V_{animal}$), as in (Luo *et al*, 2003), where L_{vgll3}, E_{vgll3}, L_{six6} and E_{six6} denotes frequency of L and E alleles in *vgll3* and *six6* loci, respectively, β_{vgll3} and β_{six6} denotes *six6* and *vgll3* E to L substitution effects, respectively, and se denotes standard error of the estimate. Percent repeatability for each model is calculated as $R = V_{ID} / (V_{ID} + V_{error}) * 100$, and heritability values were calculated as $h^2 = V_{animal} / (V_{animal} + V_{tank} + V_{ID})$, where V_{tank}, V_{ID}, and V_{error} are the model variance estimates associated with tank (ε_{tank}), individual (ε_{ID}), and error (ε_{error}) terms in $Model_{VA.full}$. Similarly, evolvability (I_A) was calculated as $V_A / \bar{y}^2$ using $Model_{VA.full}$, where $\bar{y}$ is the mean trait value (Hansen *et al*, 2011; Houle, 1992). Evolvabilities are interpreted as expected proportional responses in the trait mean under unit selection (i.e. the selection on fitness itself) (Hansen *et al*, 2003; Hansen *et al*, 2011). For all variance components, 95% confidence intervals were estimated by obtaining the posterior distributions of random effect terms in the model ($Model_{VA.full}$), using the *sims* function in the arm package(version 1.1.4-4, Gelman and Su, 2020)) in R, using 10,000 permutations. The simulations generate 10000 estimates for random effect terms, which then used to calculate the variance components as above, sorted, with 250th and 9750th estimates are recorded as 95% CIs. We did not control for the effect of dominance in the analyses, which may have inflated the estimates of additive genetic variance (Lynch and Walsh, 1998).

Results:

Shape analysis:

The multivariate analyses using Procrustes shape variation as the response showed that genetic variation in *six6*, but not in *vgll3* is associated with shape change in the body plane (Table 2). The change in the body plane appears to be related to changes in the head region associated with *six6*, whereby a substitution from $six6^E$ to $six6^L$ elongates the head and slightly bends up the lateral body positioning at ends of the lateral line, while $vgll3^E$ to $vgll3^L$ substitution reduces the head area relatively to the body area, and pushes the anterior anal fin landmark toward the posterior end of the body plane (Figure 1a). On the other hand, the genetic variation in *vgll3* and *six6* are not associated with overall shape changes in small and large cross sections. Although not statistically significant, a $vgll3^E$ to $vgll3^L$ substitution was linked with a narrower horizontal width, a smaller aerobic muscle area in the small cross section (Figure 1b), and a narrower aerobic muscle extension perpendicular to lateral line in the large cross section (Figure 1c). These results seem to be concordant with the trait-based analysis (see below). Overall, family, tank, feed restriction, and length were important determinants

275 for shape variation in all planes, and condition factor was also significant in the analysis of the body plane
276 (Table 2).

277 <u>*Trait analysis:*</u> After correcting for body length, condition factor, feed restriction, and sex, out of 21
278 morphological traits, nine and four were statistically significantly associated with the *vgll3* and *six6* loci,
279 respectively (Table 1, Figure 2. See also Supplementary Table 3 for *t*-values and effective degrees of freedoms
280 of terms). In general, the *vgll3*^{E} to *vgll3*^{L} substitution effect decreased trait values (Table 1, Figure 2) with
281 changes in trait values between *vgll3*^{EE} and *vgll3*^{LL} genotypes being > 1 %, and up to 3 % of the mean trait
282 values (Figure 2). Notably, aerobic muscle depth in the small cross section was reduced by 3.45 % (p< 0.001)
283 and aerobic muscle vertical extension in the large cross section was reduced by 2.72 % (p= 0.006) by the *vgll3*^{E}
284 to *vgll3*^{L} allelic substitution (Table 1, Figure 2). The *vgll3* allelic substitution effect associated with lateral red
285 muscle length was statistically significant when three aerobic muscles trait values were combined into one
286 composite value (p< 0.001, Supplementary Table 4). The *vgll3*^{L} allele also decreased vertebral thickness in both
287 small (1.37 % decrease, p= 0.009) and large (1.21 % decrease, p= 0.032) cross sections (Table 1, Figure 2). The
288 *vgll3*^{E} to *vgll3*^{L} substitution effect significantly reduced the small cross section diameter by 1.43 % (p= 0.012),
289 whereas the small section centroid size was reduced by 0.86 % (p= 0.012, Table 1, Figure 2). Reduced eye
290 diameter, snout length, and the anal fin length was also associated with the *vgll3*^{L} allele (Table 1, Figure 2). The
291 trait values for all ray fins (dorsal, anal, pectoral, and tail fins) was trending toward a smaller size in relation to
292 the late maturing genotype (Table 1, Figure 2), and their cumulative effect, i.e., effect size of all trait values
293 combined, was statistically significant (p= 0.022, Supplementary Table 4). We observed that in some traits the
294 variation explained by *vgll3*^{E} to *vgll3*^{L} substitution in *six6* and *vgll3* loci was up to 50% of the variation explained
295 by length (a factor with strong, positive allometric effect on other trait values, see Table 1), suggesting that this
296 variation is biologically important (Supplementary Figure 4).

297 Most differences explained by variation in the *six6* genomic region were related to changes in head and body
298 size. As such, the *six6*^{E} to *six6*^{L} substitution was associated with a 0.17 % decrease on body centroid (t= -3.70,
299 p< 0.001) and a 0.47 % increase on head centroid size (t= 2.68, p= 0.008, Table 1, Figure 2). Finally, the snout
300 length, measured as the distance between the center of the eye and maximum anterior point in the body, was
301 elongated by 0.73 % in fish with an additional *six6*^{L} allele (t= 3.05, p= 0.002, Table 1, Figure 2).

302 Sex effects typically ranged from smaller and up to the same order of magnitude as the allele substitution
303 effects in the life-history loci (Table 1). Notably, the snout, pectoral fin, and anal fin were significantly larger in
304 males compared to the females (p= 0.002, p= 0.007, and p= 0.021, respectively. Table 1). In addition, the head
305 centroid was larger in males compared to females (p= 0.040, Table 1). As expected length was a strong

predictor of all traits and condition factor was also positively associated with most of the traits (Table 1). Feed restriction was notably associated with decrease in fin trait values, such as dorsal fin ($p < 0.001$), anal fin ($p = 0.040$), and tail fin ($p = 0.003$, Table 1). Interestingly, feed restriction substantially reduced the centroid size ($p = 0.011$), cross section diameter ($p = 0.003$), and the size of the aerobic muscle ($p = 0.005$) in the small cross section, but not in the large cross section (Table 1).

Trait heritabilities were low to moderate in most cases, with a mean heritability of 0.19 across all 21 traits (Table 3). Length of tail fin and body centroid size exhibited the highest heritability with 0.50 (95 % CI 0.47-0.54) and 0.47 (95 % CI 0.43-0.50), followed by pectoral fin with 0.41 (95 % CI 0.36-0.45). The repeatability of trait measurements was moderate (mean repeatability 73.0 %, Table 1).

Evolvabilities (mean-scaled additive genetic variances, denoted as I_A) differed greatly among traits (Table 3). Interestingly, body centroid size had the lowest evolvability (<0.001), meaning that under selection as strong as fitness itself (unit selection) the expected increase in this trait would be less than 0.1%. On the other hand, large cross section aerobic muscle had an evolvability as high as 0.72, meaning that the expected increase in this trait under strong selection could be as high as 71% of the mean trait value. In general, out of 21 traits measured, aerobic muscle and vertebrae thickness traits had higher I_A, while centroid sizes and cross-section diameters had lower I_A (Table 3).

Additive genetic variation explained by *vgll3* locus was non-zero for 12 traits (Table 3). Consistent with the fixed effect parameterization of the genotype, a substantial portion of the additive genetic variation in vertebra thickness was explained by *vgll3*, with 30.7 % and 13.0 % for small and large cross sections, respectively (Table 3). A significant portion of the additive genetic variation in small section aerobic muscle, cross section diameter, and body centroid was also explained by the *vgll3* locus, with 22.4 %, 12.7, and 6.3 % for each trait, respectively (Table 3). The contribution of *six6* locus to additive genetic variation associated included snout length (9.4 %), and head and body centroid size (5.2 % and 4.2 %, respectively, Table 3) consistent with the locus effect size.

As length is a strong a predictor of both trait values, and overall body shape, a spurious association between traits and the life-history loci may be expected if these loci affect trait values via length as a mediator. To test this, we constructed a model to include interaction between length and life-history loci. Across 21 traits, we did not observe a meaningful difference in main genetic effects, nor were interaction terms *t*-values substantial (Supplementary Figure 5), suggesting that length-by-genotype interaction did not drive the estimated relations.

Discussion

Intraspecific differences in functionally important morphological traits may provide important insights into the mechanistic basis of adaptation. We detected several morphological traits in juvenile Atlantic salmon that were linked with variation in genomic regions that were previously reported to be associated with life-history diversity and known to be under local selection. The genetic polymorphism in the *vgll3* locus appears to shape a suite of traits that are associated with swimming performance, while the genetic polymorphism in the *six6* locus shapes head and body size, and head features such as snout length, which potentially affects resource acquisition efficiencies for different foraging strategies. On the other hand, these genomic regions have only a small effect on the general shape of the morphological planes. The only statistically significant effect was detected in the body plane plan that was associated with the *six6* loci (Figure 1), for which the change in shape appears to be concordant with change in head/body proportions observed in the univariate trait analysis. Our results support these genomic regions having broad phenotypic effects, which may have emerged from either a form of pleiotropy or due to linkage disequilibrium. Our design does not allow to categorize the pleiotropic effects further, whether it is based on an effect of single causal variant (biological pleiotropy), or based on effects associated with different phenotypes along a biochemical pathway (mediated pleiotropy), or as a result of linkage disequilibrium between two independent causative loci (spurious pleiotropy, e.g., Solovieff *et al*, 2013). Yet, the strong genetic interdependence among traits associated with *six6* and *vgll3* may have a developmental origin, which is supported by the patterns of expression of genes in these genomic regions during development, and their molecular regulatory functions, (Ahi *et al*, 2022; Kurko *et al*, 2020; Mobley *et al*, 2021; Moustakas-Verho *et al*, 2020; Verta *et al*, 2020; Verta *et al*, 2024).

The suite of morphological traits associated with *vgll3* variation reflects changes along a functional axis that facilitates efficient cruising and steady swimming (*vgll3*^{E}) versus maneuvering and acceleration (*vgll3*^{L}). Efficient cruising is an important trait especially in the marine environment, while better maneuvering and acceleration help to better cope with biotic (i.e. competition and predation risk) and abiotic (flow regime) factors in the freshwater habitat. The larger aerobic muscle area associated with the *vgll3*^{E} allele could indicate a higher potential for aerobic muscle activity. This result is in concordance with (Prokkola *et al*, 2022) who demonstrated that the juvenile Atlantic salmon with early maturing genotype has a higher maximum metabolic rate (MMR) and aerobic scope (AS). Aerobic locomotion is expected to be central for Atlantic salmon during the marine phase, where salmon sub-adults migrate and continuously forage for food. Our results suggests salmon with the early genotype are more likely to maintain sustained swimming and foraging activities, beneficial during marine exploration. On the other hand, it is not clear if the genetic association between life-history loci

367 and morphological traits persists between life stages. The parr-smolt transformation (smoltification) includes
368 morphological changes that would prepare juvenile Atlantic salmon for the marine environment (Jonsson and
369 Jonsson, 2011b), hence phenotype-genotype association might be different either as a result of smoltification
370 or change in the environment (Aguirre *et al*, 2014). However, since individuals used in this study have a
371 complete or close to complete smolt phenotype, conclusions may be more relevant to the marine compared to
372 the freshwater life stage.

373 Increased vertebral thickness associated with the *vgll3*^{E} allele could provide stiffness for energy efficient
374 undulation movement during steady swimming (Donatelli *et al*, 2021), though it may come at the expense of
375 body flexibility that may facilitate piscivorous prey capture. A larger aerobic muscle area and thicker vertebra
376 may eventually facilitate earlier maturation via more energy efficient resource acquisition at sea, suggesting
377 that local adaptation for optimal age structure could be partly mediated by conditions at sea. Hence, while our
378 results do not explain causation of early male maturation in fresh water, we cannot explicitly rule out that the
379 link between *vgll3* and age at maturity is mediated via its effect on body shape. Sex was also an important
380 factor shaping the trait variation. Intriguingly, significant change in shape associated with sex and *vgll3*
381 genotype was also in concordant with respect to maturation timing. As such, males, which on average mature
382 earlier than females, and *vgll3* allele associated with early maturation had similar direction of change in these
383 morphological traits.

384 Larger fin sizes in fish increase maneuverability and stability (Webb, 1984), and correspondingly in Atlantic
385 salmon larger fins occur in populations that occupy faster flowing streams (Riddell and Leggett, 1981). Overall,
386 we found that the ray-fins of fish were consistently larger for the *vgll3*^{E} allele than the *vgll3*^{L} allele
387 (Supplementary Table 4). However, this improvement for maneuverability and stability may come in the
388 expense of efficiency in longer marine migrations, as a result of increased drag. For example, in coho salmon,
389 juveniles of inland population with longer migration distances have smaller fins (Taylor and McPhail, 1985),
390 which may help to reduce drag in long migrations (Dynes *et al*, 2005; Varian and Nichols, 2010). A larger cross
391 section diameter and larger fin lengths associated with the *vgll3*^{E} allele likely facilitate maneuvering at the
392 expense of efficient cruising, which is in contrast to the *vgll3*^{E} effect that increases aerobic muscle area and
393 vertebral thickness. Similarly, the slender body (a smaller cross section diameter) associated with *vgll3*^{L} is
394 consistent with minimizing the drag for cruising body-form (e.g., Webb, 1988), advantageous for a multi-sea
395 winter strategy that migrates longer distances in the ocean (e.g., O'Sullivan *et al*, 2022). On the other hand, the
396 direction of effect on fin size associated with *vgll3*^{E} *to vgll3*^{L} substitution is concordant with the effect of
397 restricted-food regime, suggesting that the allelic substation effect may be correlated to food limitation

conditions. Thus overall, the direction of *vgll3* genetic effects are not functionally consistent in relation to proposed ecological roles of these morphological traits.

The changes associated with the genetic variation in *six6* locus that are affecting body and head sizes are linked to ecological processes related to resource acquisition mechanisms. A larger head (and a smaller body) associated with the *six6*^{L} allele and larger snout length may be associated with feeding regime towards piscivory (Keeley *et al*, 2005), or generally consuming larger prey items. This interpretation corroborates with the study by Aykanat *et al* (2020), in which fish with *six6*^{LL} genotype were shown to be more efficient in resource acquisition than fish with *six6*^{EE} genotype.

Evolvabilities (I_A) ranged from normal to very high compared to a recent meta-analysis (Hansen *et al*, 2011). The median evolvability for length traits is 0.001 (or 0.1%, Hansen and Pélabon, 2021; Hansen *et al*, 2011). Normal evolvability values were found for centroid sizes and cross-section diameters, while aerobic muscle and vertebrae thickness had high evolvabilities, suggesting that these traits could evolve rapidly in response to selection induced by environmental change. Interestingly, a substantial portion of the additive genetic variation associated with some traits, such as aerobic muscle area and vertebrate thickness, was explained by the *vgll3* locus, suggesting the locus' importance in shaping the additive genetic landscape.

Taken together, *vgll3* and *six6* loci have complex associations with morphology. These do not consistently align with adaptive differences between early- and late-maturation genotypes associated with marine migration, but could be important e.g., during spawning where higher maneuverability of smaller males may be beneficial for reproductive success, or in early life stages. On the other hand, it is also plausible that these changes are genetically correlated as part of broad changes during development, and that some of which have potentially maladaptive consequences. In fact, when traits are genetically correlated, the cumulative adaptive value of trait values cannot be optimal (Schluter, 1996), since breaking suboptimal trait combinations that are genetically correlated may be challenging for evolution (Blows, 2007).

It is important to recognize that extrapolation to the marine stage of Atlantic salmon based on juvenile morphology may have limitations. It is unknown if the genotype-associated morphological variation is correlated between juvenile and adult stages. While there may be genetic correlation between freshwater and marine environments (Fleming *et al*, 1994; Morinville and Rasmussen, 2006; Taylor and McPhail, 1985), the morphological changes associated with adaption to the marine environment, the parr-smolt transformation (smoltification) may break apart trait correlations, similar to how metamorphosis takes places many animal taxa (e.g., Aguirre *et al*, 2014). Since the data in this study were composed of individuals that had completed the parr-smolt transformation, or are close to completion, conclusions are likely more relevant to marine

429 stages than the freshwater stages. However, any adaptive inference associated with a specific life stage should
430 be taken with caution, until observed patterns are further tested and verified at different life stages. Finally,
431 while it is reasonable to hypothesize that the observed *vgll3* and *six6* associated morphological variation is
432 adaptively important, the fitness effects of this variation should be better assessed before any evolutionary
433 conclusions can be made (Kingsolver *et al*, 1995).

434 In conclusion, we have detected substantial morphological variation associated with two genomic regions
435 which are also major determinants of life-history variation and known to be under local selection. These loci
436 appear to influence multiple, strongly correlated traits, suggestive of a broad regulatory role with impacts
437 across the whole life cycle. How these genetic correlations are shaped – via single locus pleiotropy or close
438 physical linkage of multiple genes – remains to be determined.

439

440 Acknowledgment

441 We thank Artur Porto for discussion related to morphometric analyses, and Annukka Ruokolainen, Seija
442 Tillanen, Andrew H. House, Jacqueline E. Moustakas-Verho, Nikolai Piavchenko for helps with sampling. This
443 work was supported by the Research Council of Finland (grant nos. 328860, 353388, and 325964 to TA, and
444 314254, 314255, 327255 and 342851 to CRP), and the European Research Council under the European Articles
445 Union's Horizon 2020 and Horizon Europe research and innovation programs (grant no. 742312 and 101054307
446 to CRP). Views and opinions expressed are however those of the author(s) only and do not necessarily reflect
447 those of the European Union or the European Research Council Executive Agency. Neither the European Union
448 nor the granting authority can be held responsible for them. LG was supported by Erasmus+ programme. The
449 authors declare no competing interests.

450

451 Ethical approval

452 The experiments were approved by the Project Authorisation Board (ELLA) on behalf of the Regional
453 Administrative Agency for Southern Finland (ESAVI) under experimental license ESAVI/2778/2018.

454

455

Author contributions

TA, VLP, and GHB conceptualized the paper. TA analyzed the data with significant input from GHB and PVD. SJ and LG performed landmarkings. JE, and CRP oversaw the resources and infrastructure. PVD and CRP devised the breeding design and reared the fish. TA and PVD sampled the fish and digitized the images. TA drafted the MS with significant inputs from PVD, VLP, and GHB, and all coauthors contributed to subsequent drafts.

References:

Aguirre JD, Blows MW, Marshall DJ (2014). The genetic covariance between life cycle stages separated by metamorphosis. *Proceedings Biological sciences / The Royal Society* **281**(1788)**:** 20141091.

Ahi EP, Sinclair-Waters M, Moustakas-Verho J, Jansouz S, Primmer CR (2022). Strong regulatory effects of *vgll3* genotype on reproductive axis gene expression in juvenile male Atlantic salmon. *Gen Comp Endocrinol* **325:** 114055.

Altringham JD, Ellerby DJ (1999). Fish swimming: patterns in muscle function. *J Exp Biol* **202**(Pt 23)**:** 3397-3403.

Archambeault SL, Bartschi LR, Merminod AD, Peichel CL (2020). Adaptation via pleiotropy and linkage: Association mapping reveals a complex genetic architecture within the stickleback *Eda* locus. *Evol Lett* **4**(4)**:** 282-301.

Asheim ER, Debes PV, House A, Liljestrom P, Niemela PT, Siren JP *et al* (2023). Atlantic salmon (*Salmo salar*) age at maturity is strongly affected by temperature, population and age-at-maturity genotype. *Conserv Physiol* **11**(1)**:** coac086.

Aykanat T, McLennan D, Metcalfe NB, Prokkola JM (2024). Early survival in Atlantic salmon is associated with parental genotypes at loci linked to timing of maturation. *Evolution* **78**(8)**:** 1441-1452.

Aykanat T, Ozerov M, Vaha JP, Orell P, Niemela E, Erkinaro J *et al* (2019). Co-inheritance of sea age at maturity and iteroparity in the Atlantic salmon *vgll3* genomic region. *J Evol Biol* **32**(4)**:** 343-355.

Aykanat T, Rasmussen M, Ozerov M, Niemela E, Paulin L, Vaha JP *et al* (2020). Life-history genomic regions explain differences in Atlantic salmon marine diet specialization. *J Anim Ecol* **89**(11)**:** 2677-2691.

Ayllon F, Kjaerner-Semb E, Furmanek T, Wennevik V, Solberg MF, Dahle G *et al* (2015). The *vgll3* locus controls age at maturity in wild and domesticated Atlantic salmon (*Salmo salar* L.) Males. *PLoS Genet* **11**(11)**:** e1005628.

Baken EK, Collyer ML, Kaliontzopoulou A, Adams DC (2021). geomorph v4.0 and gmShiny: Enhanced analytics and a new graphical interface for a comprehensive morphometric experience. *Methods in Ecology and Evolution* **12**(12)**:** 2355-2363.

Bangura PB, Tiira K, Niemela PT, Erkinaro J, Liljestrom P, Toikkanen A *et al* (2022). Linking *vgll3* genotype and aggressive behaviour in juvenile Atlantic salmon (*Salmo salar*). *J Fish Biol* **100**(5)**:** 1264-1271.

Barrett RD, Hoekstra HE (2011). Molecular spandrels: tests of adaptation at the genetic level. *Nat Rev Genet* **12**(11)**:** 767-780.

Barson NJ, Aykanat T, Hindar K, Baranski M, Bolstad GH, Fiske P *et al* (2015). Sex-dependent dominance at a single locus maintains variation in age at maturity in salmon. *Nature* **528**(7582)**:** 405-408.

Bates DM (2010). lme4: Mixed-effects modeling with R.

Baxter D, Cohen KE, Donatelli CM, Tytell ED (2022). Internal vertebral morphology of bony fishes matches the mechanical demands of different environments. *Ecology and evolution* **12**(11)**:** e9499.

Blows MW (2007). A tale of two matrices: multivariate approaches in evolutionary biology. *J Evol Biol* **20**(1)**:** 1-8.

Boyle EA, Li YI, Pritchard JK (2017). An Expanded View of Complex Traits: From Polygenic to Omnigenic. *Cell* **169**(7)**:** 1177-1186.

Chan YF, Marks ME, Jones FC, Villarreal G, Jr., Shapiro MD, Brady SD *et al* (2010). Adaptive evolution of pelvic reduction in sticklebacks by recurrent deletion of a *Pitx1* enhancer. *Science* **327**(5963)**:** 302-305.

Collyer ML, Adams DC, Freckleton R (2018). RRPP: An R package for fitting linear models to high-dimensional data using residual randomization. *Methods in Ecology and Evolution* **9**(7)**:** 1772-1779.

Colosimo PF, Hosemann KE, Balabhadra S, Villarreal G, Jr., Dickson M, Grimwood J *et al* (2005). Widespread parallel evolution in sticklebacks by repeated fixation of Ectodysplasin alleles. *Science* **307**(5717)**:** 1928-1933.

Crossin GT, Hinch SG, Farrell AP, Higgs DA, Lotto AG, Oakes JD *et al* (2004). Energetics and morphology of sockeye salmon: effects of upriver migratory distance and elevation. *J Fish Biol* **65**(3)**:** 788-810.

Debes PV, Piavchenko N, Erkinaro J, Primmer CR (2020). Genetic growth potential, rather than phenotypic size, predicts migration phenotype in Atlantic salmon. *Proceedings Biological sciences / The Royal Society* **287**(1931)**:** 20200867.

Debes PV, Piavchenko N, Ruokolainen A, Ovaskainen O, Moustakas-Verho JE, Parre N *et al* (2019). Large single-locus effects for maturation timing are mediated via condition variation in Atlantic salmon. *bioRxiv*: 780437 (v780433).

Debes PV, Piavchenko N, Ruokolainen A, Ovaskainen O, Moustakas-Verho JE, Parre N *et al* (2021). Polygenic and major-locus contributions to sexual maturation timing in Atlantic salmon. *Mol Ecol* **30**(18): 4505-4519.

Donatelli CM, Roberts AS, Scott E, DeSmith K, Summers D, Abu-Bader L *et al* (2021). Foretelling the Flex-Vertebral Shape Predicts Behavior and Ecology of Fishes. *Integr Comp Biol* **61**(2): 414-426.

Dynes J, Magnan P, Bernatchez L, Rodríguez MA (2005). Genetic and morphological variation between two forms of lacustrine brook charr. *J Fish Biol* **54**(5): 955-972.

Eliason EJ, Farrell AP (2015). Oxygen uptake in Pacific salmon *Oncorhynchus* spp.: when ecology and physiology meet. *J Fish Biol*.

Elmer KR, Kusche H, Lehtonen TK, Meyer A (2010). Local variation and parallel evolution: morphological and genetic diversity across a species complex of neotropical crater lake cichlid fishes. *Philosophical transactions of the Royal Society of London Series B, Biological sciences* **365**(1547): 1763-1782.

Endler JA (2000). Adaptive Genetic Variation in the Wild. In: Mousseau TA, SinerVo B and Endler JA (eds) *Adaptive Genetic Variation in the Wild*. Oxford University Press.

Ferry-Graham LA, Bolnick DI, Wainwright PC (2002). Using functional morphology to examine the ecology and evolution of specialization. *Integr Comp Biol* **42**(2): 265-277.

Fitzgerald DB, Winemiller KO, Sabaj Pérez MH, Sousa LM, Seymour C (2017). Using trophic structure to reveal patterns of trait-based community assembly across niche dimensions. *Funct Ecol* **31**(5): 1135-1144.

Fleming IA, Jonsson B, Gross MR (1994). Phenotypic Divergence of Sea-ranched, Farmed, and Wild Salmon. *Can J Fish Aquat Sci* **51**(12): 2808-2824.

Gelman A, Su YS (2020). arm: Data Analysis Using Regression and Multilevel/Hierarchical Models. R package version 1.11-2.

Gower JC (1975). Generalized procrustes analysis. *Psychometrika* **40**(1): 33-51.

Hansen TF, Pélabon C (2021). Evolvability: A Quantitative-Genetics Perspective. *Annual Review of Ecology, Evolution, and Systematics* **52**(1): 153-175.

572 Hansen TF, Pelabon C, Armbruster WS, Carlson ML (2003). Evolvability and genetic constraint in Dalechampia
573 blossoms: components of variance and measures of evolvability. *J Evol Biol* **16**(4)**:** 754-766.

574

575 Hansen TF, Pélabon C, Houle D (2011). Heritability is not Evolvability. *Evolutionary Biology* **38**(3)**:** 258-277.

576

577 Hoar WS (1988). 4 The Physiology of Smolting Salmonids. In: Hoar WS and Randall DJ (eds) *Fish Physiology*.
578 Academic Press. Vol. 11, pp 275-343.

579

580 Houle D (1992). Comparing evolvability and variability of quantitative traits. *Genetics* **130:** 195-204.

581

582 Jakobson CM, Jarosz DF (2020). What Has a Century of Quantitative Genetics Taught Us About Nature's Genetic
583 Tool Kit? *Annu Rev Genet* **54:** 439-464.

584

585 Jimenez-Gomez JM, Wallace AD, Maloof JN (2010). Network analysis identifies *ELF3* as a QTL for the shade
586 avoidance response in Arabidopsis. *PLoS Genet* **6**(9)**:** e1001100.

587

588 Jonsson B, Jonsson N (2011a). *Ecology of Atlantic salmon and brown trout : habitat as a template for life*
589 *histories*. Springer: Dordrecht.

590

591 Jonsson B, Jonsson N (2011b). Ecology of salmon and trout 2011.

592

593 Kawecki TJ, Ebert D (2004). Conceptual issues in local adaptation. *Ecol Lett* **7**(12)**:** 1225-1241.

594

595 Keeley ER, Parkinson EA, Taylor EB (2005). Ecotypic differentiation of native rainbow trout (*Oncorhynchus*
596 *mykiss*) populations from British Columbia. *Can J Fish Aquat Sci* **62**(7)**:** 1523-1539.

597

598 Kingsolver JG, Woods HA, Gilchrist G (1995). Traits related to fitness. *Science* **267**(5196)**:** 396.

599

600 Klingenberg CP (2016). Size, shape, and form: concepts of allometry in geometric morphometrics. *Dev Genes*
601 *Evol* **226**(3)**:** 113-137.

602

603 Kurko J, Debes PV, House AH, Aykanat T, Erkinaro J, Primmer CR (2020). Transcription Profiles of Age-at-
604 Maturity-Associated Genes Suggest Cell Fate Commitment Regulation as a Key Factor in the Atlantic Salmon
605 Maturation Process. *G3* **10**(1)**:** 235-246.

606

607 Kuznetsova A, Brockhoff PB, Christensen RHB (2017). lmerTest Package: Tests in Linear Mixed Effects Models. *J*
608 *Stat Softw* **82**(13).

609

610 Long JH, Nipper KS (1996). The Importance of Body Stiffness in Undulatory Propulsion. *Am Zool* **36**(6)**:** 678-694.

Lundsgaard-Hansen B, Matthews B, Vonlanthen P, Taverna A, Seehausen O (2013). Adaptive plasticity and genetic divergence in feeding efficiency during parallel adaptive radiation of whitefish (*Coregonus* spp.). *J Evol Biol* **26**(3)**:** 483-498.

Luo L, Mao Y, Xu S (2003). Correcting the bias in estimation of genetic variances contributed by individual QTL. *Genetica* **119**(2)**:** 107-113.

Lynch M, Walsh B (1998). *Genetics and analysis of quantitative traits*. Sinauer Associates: Sunderland, MA.

Mackay TF, Stone EA, Ayroles JF (2009). The genetics of quantitative traits: challenges and prospects. *Nat Rev Genet* **10**(8)**:** 565-577.

Miettinen A, Dannewitz J, Palm S, Ahi EP, Romakkaniemi A, Vähä V *et al* (2023). Loci associated with maturation, migration and appetite control are linked with signals of fine-scale local selection in a large Atlantic salmon population. *bioRxiv***:** 2023.2008.2023.553800.

Mindel BL, Neat FC, Trueman CN, Webb TJ, Blanchard JL (2016). Functional, size and taxonomic diversity of fish along a depth gradient in the deep sea. *PeerJ* **4:** e2387.

Mobley KB, Aykanat T, Czorlich Y, House A, Kurko J, Miettinen A *et al* (2021). Maturation in Atlantic salmon (*Salmo salar*, Salmonidae): a synthesis of ecological, genetic, and molecular processes. *Rev Fish Biol Fish* **31**(3)**:** 523-571.

Morinville GR, Rasmussen JB (2006). Does life-history variability in salmonids affect habitat use by juveniles? A comparison among streams open and closed to anadromy. *J Anim Ecol* **75**(3)**:** 693-704.

Morinville GR, Rasmussen JB (2007). Distinguishing between juvenile anadromous and resident brook trout (Salvelinus fontinalis) using morphology. *Environ Biol Fishes* **81**(2)**:** 171-184.

Moustakas-Verho JE, Kurko J, House AH, Erkinaro J, Debes P, Primmer CR (2020). Developmental expression patterns of *six6*: A gene linked with spawning ecotypes in Atlantic salmon. *Gene Expr Patterns* **38:** 119149.

Nielsen EE, Hemmer-Hansen J, Larsen PF, Bekkevold D (2009). Population genomics of marine fishes: identifying adaptive variation in space and time. *Mol Ecol* **18**(15)**:** 3128-3150.

O'Sullivan RJ, Ozerov M, Bolstad GH, Gilbey J, Jacobsen JA, Erkinaro J *et al* (2022). Genetic stock identification reveals greater use of an oceanic feeding ground around the Faroe Islands by multi-sea winter Atlantic salmon, with variation in use across reporting groups. *ICES J Mar Sci* **79**(9)**:** 2442-2452.

Olson-Manning CF, Wagner MR, Mitchell-Olds T (2012). Adaptive evolution: evaluating empirical support for theoretical predictions. *Nat Rev Genet* **13**(12)**:** 867-877.

Orr HA (2000). Adaptation and the cost of complexity. *Evolution* **54**(1)**:** 13-20.

Otto SP (2004). Two steps forward, one step back: the pleiotropic effects of favoured alleles. *Proceedings Biological sciences / The Royal Society* **271**(1540)**:** 705-714.

Paaby AB, Rockman MV (2013). The many faces of pleiotropy. *Trends Genet* **29**(2)**:** 66-73.

Peris Tamayo AM, Devineau O, Praebel K, Kahilainen KK, Ostbye K (2020). A brain and a head for a different habitat: Size variation in four morphs of Arctic charr (*Salvelinus alpinus* (L.)) in a deep oligotrophic lake. *Ecology and evolution* **10**(20)**:** 11335-11351.

Porto A, Voje KL, Price S (2020). ML-morph: A fast, accurate and general approach for automated detection and landmarking of biological structures in images. *Methods in Ecology and Evolution* **11**(4)**:** 500-512.

Pritchard VL, Makinen H, Vaha JP, Erkinaro J, Orell P, Primmer CR (2018). Genomic signatures of fine-scale local selection in Atlantic salmon suggest involvement of sexual maturation, energy homeostasis and immune defence-related genes. *Mol Ecol* **27**(11)**:** 2560-2575.

Prokkola JM, Asheim ER, Morozov S, Bangura P, Erkinaro J, Ruokolainen A *et al* (2022). Genetic coupling of life-history and aerobic performance in Atlantic salmon. *Proceedings Biological sciences / The Royal Society* **289**(1967)**:** 20212500.

Proulx R, Magnan P (2004). Contribution of phenotypic plasticity and heredity to the trophic polymorphism of lacustrine brook charr (*Salvelinus fontinalis* M.). *Evol Ecol Res* **6**(4)**:** 503-522.

R Core Team. (2019). R Foundation for Statistical Computing, Vienna, Austria.

Riddell BE, Leggett WC (1981). Evidence of an adaptive basis for geographic variation in body morphology and time of downstream migration of juvenile Atlantic salmon (*Salmo salar*). *Can J Fish Aquat Sci* **38**(3)**:** 308-320.

Schluter D (1996). Ecological causes of adaptive radiation. *Am Nat*.

Shuman JL, Coughlin DJ (2018). Red muscle function and thermal acclimation to cold in rainbow smelt, *Osmerus mordax*, and rainbow trout, *Oncorhynchus mykiss*. *J Exp Zool A Ecol Integr Physiol* **329**(10)**:** 547-556.

Simonsen MK, Siwertsson A, Adams CE, Amundsen PA, Praebel K, Knudsen R (2017). Allometric trajectories of body and head morphology in three sympatric Arctic charr (*Salvelinus alpinus* (L.)) morphs. *Ecology and evolution* **7**(18)**:** 7277-7289.

Sinclair-Waters M, Odegard J, Korsvoll SA, Moen T, Lien S, Primmer CR *et al* (2020). Beyond large-effect loci: large-scale GWAS reveals a mixed large-effect and polygenic architecture for age at maturity of Atlantic salmon. *Genet Sel Evol* **52**(1)**:** 9.

Snorrason S (1994). Trophic specialization in Arctic charr *Salvelinus alpinus* (Pisces; Salmonidae): morphological divergence and ontogenetic niche shifts. *Biol J Linn Soc* **52**(1)**:** 1-18.

Solovieff N, Cotsapas C, Lee PH, Purcell SM, Smoller JW (2013). Pleiotropy in complex traits: challenges and strategies. *Nat Rev Genet* **14**(7)**:** 483-495.

Svanbäck R, Eklöv P (2003). Morphology dependent foraging efficiency in perch: a trade-off for ecological specialization? *Oikos* **102**(2)**:** 273-284.

Taylor EB, McPhail JD (1985). Variation in body morphology among british columbia populations of coho salmon, *Oncorhynchus kisutch*. *Can J Fish Aquat Sci* **42**(12)**:** 2020-2028.

Varian A, Nichols KM (2010). Heritability of morphology in brook trout with variable life histories. *PLoS One* **5**(9)**:** e12950.

Vazquez AI, Bates DM, Rosa GJ, Gianola D, Weigel KA (2010). Technical note: an R package for fitting generalized linear mixed models in animal breeding. *J Anim Sci* **88**(2)**:** 497-504.

Verta JP, Debes PV, Piavchenko N, Ruokolainen A, Ovaskainen O, Moustakas-Verho JE *et al* (2020). Cis-regulatory differences in isoform expression associate with life history strategy variation in Atlantic salmon. *PLoS Genet* **16**(9)**:** e1009055.

Verta JP, Moustakas-Verho JE, Donner I, Frapin M, Ruokolainen A, Debes PV *et al* (2024). A complex mechanism translating variation of a simple genetic architecture into alternative life histories. *Proc Natl Acad Sci U S A* **121**(48)**:** e2402386121.

Wagner GP, Altenberg L (1996). Perspective: Complex Adaptations and the Evolution of Evolvability. *Evolution* **50**(3)**:** 967-976.

Wagner GP, Zhang J (2011). The pleiotropic structure of the genotype-phenotype map: the evolvability of complex organisms. *Nat Rev Genet* **12**(3)**:** 204-213.

Webb PW (1984). Body form, locomotion and foraging in aquatic vertebrates. *Am Zool* **24**(1)**:** 107-120.

730
731 Webb PW (1988). Simple physical principles and vertebrate aquatic locomotion. *Am Zool* **28**(2)**:** 709-725.

732
733 Weith M, Grossbach J, Clement-Ziza M, Gillet L, Rodriguez-Lopez M, Marguerat S *et al* (2023). Genetic effects
734 on molecular network states explain complex traits. *Mol Syst Biol* **19**(8)**:** e11493.

735
736 Ziyatdinov A, Vazquez-Santiago M, Brunel H, Martinez-Perez A, Aschard H, Soria JM (2018). lme4qtl: linear
737 mixed models with flexible covariance structure for genetic studies of related individuals. *BMC Bioinformatics*
738 **19**(1)**:** 68.

739
740 Zueva KJ, Lumme J, Veselov AE, Primmer CR, Pritchard VL (2020). Population genomics reveals repeated signals
741 of adaptive divergence in the Atlantic salmon of north-eastern Europe. *J Evol Biol* **34**(6)**:** 866-878.

Tables (4) and Figures (2):

Table 1: Estimated fixed effect coefficients for 21 morphological traits obtained across three body planes. Trait lengths are given in centimeters (cm) for all traits. Coef. (SE) indicates coefficients and their standard error. B, S, and L in the body plane column indicates lateral view of the body, small and large cross sections, respectively. Significant *p* values are indicated with asterisk (* and ** denotes *p*<0.05 and *p*<0.01, respectively).

Trait	Body Plane[1]	Trait value formula[1]	Intercept	Length (scaled)		Condition factor (scaled)		Feed restriction (*ad libitum* to restricted)		Sex (female to male)		vgll3 (E to L)		six6 (E to L)	
			coef. (SE)	coef. (SE)	*p* value	coef. (SE)	*p* value	coef. (SE)	*p* value	coef. (SE)	*p* value	coef. (SE)	*p* value	coef. (SE)	*p* value
Dorsal fin	B	B [12:13]	2.0439 (0.0305)	0.1560 (0.0064)	<0.001**	-0.0016 (0.0041)	0.696	-0.1222 (0.0176)	<0.001**	0.0228 (0.0124)	0.067	-0.0246 (0.0148)	0.106	-0.0142 (0.0126)	0.263
Anal fin	B	B [16:17]	1.35902 (0.0164)	0.06636 (0.0041)	<0.001**	0.00043 (0.0038)	0.909	-0.02549 (0.0094)	0.0402*	0.01759 (0.0076)	0.021*	-0.01979 (0.0077)	0.017*	0.00658 (0.0075)	0.378
Pectoral fin	B	B [10:11]	2.0973 (0.0202)	0.1148 (0.0029)	<0.001**	0.0082 (0.0022)	<0.001**	-0.0376 (0.0151)	0.059	0.0143 (0.0053)	0.007**	-0.0102 (0.0096)	0.29	0.0030 (0.0058)	0.601
Tail fin	B	B [19:20]	8.3e-01 (0.0098)	4.1e-02 (0.0015)	<0.001**	-8.2e-03 (0.0013)	<0.001**	-2.1e-02 (0.0037)	0.003**	2.8e-05 (0.0027)	0.992	-4.0e-03 (0.0051)	0.432	3.1e-03 (0.0030)	0.292
Caudal peduncle	B	B [15:18]	8.7e-01 (0.00428)	6.0e-02 (0.00078)	<0.001**	1.1e-02 (0.00071)	<0.001**	1.3e-03 (0.00198)	0.529	2.3e-03 (0.00144)	0.118	-2.3e-03 (0.00219)	0.294	-6.7e-05 (0.00153)	0.965
Vertebra thickness	Sml	S [3:4]	2.4e-01 (0.00265)	1.6e-02 (0.00081)	<0.001**	1.8e-03 (0.00082)	0.0241*	2.3e-03 (0.00165)	0.172	-2.2e-03 (0.00157)	0.168	-3.3e-03 (0.00117)	0.009**	5.3e-05 (0.00138)	0.969
Vertebra thickness	Lrg	L [6:7]	0.25170 (0.00282)	0.01394 (0.00077)	<0.001**	0.00467 (0.00078)	<0.001**	-0.00238 (0.00155)	0.125	-0.00244 (0.00146)	0.096	-0.00297 (0.00131)	0.032*	0.00023 (0.00137)	0.866
Cross section diameter	Sml	S [5:7]	1.1423 (0.0136)	0.0753 (0.0027)	<0.001**	0.0134 (0.0027)	<0.001**	-0.0562 (0.0114)	0.003**	0.0020 (0.0049)	0.683	-0.0157 (0.0058)	0.012*	-0.0054 (0.0050)	0.279
Cross section diameter	Lrg	L [12:8]	2.0269 (0.0117)	0.1477 (0.0021)	<0.001**	0.0312 (0.0021)	<0.001**	0.0050 (0.0108)	0.666	0.0019 (0.0039)	0.621	-0.0047 (0.0048)	0.335	-0.0046 (0.0039)	0.248
Aerobic muscle	Sml	S [(7:8+5:6)/2]	0.17549 (0.00353)	0.01024 (0.00082)	<0.001**	0.00137 (0.00083)	0.0981	-0.01237 (0.00290)	0.0051**	0.00056 (0.00153)	0.715	-0.00557 (0.00148)	<0.001**	-0.00210 (0.00149)	0.159
Aerobic muscle	Lrg	L [(8:9+12:13)/2)	0.2349 (0.00408)	0.0185 (0.00094)	<0.001**	0.0033 (0.00094)	<0.001**	0.0070 (0.00239)	0.025*	0.0017 (0.00175)	0.34	-0.0024 (0.00195)	0.222	-0.0022 (0.00174)	0.198
Aerobic muscle vertical extension	Lrg	L [(14:15+10:11)/2]	0.879 (0.0198)	0.087 (0.0039)	<0.001**	0.026 (0.0039)	<0.001**	0.038 (0.0176)	0.0916	-0.012 (0.0073)	0.089	-0.024 (0.0081)	0.006**	0.013 (0.0072)	0.067
Eye diameter[2]	B	B [(2:3+4+5)/2]	5.5e-01 (0.00358)	2.2e-02 (0.00094)	<0.001**	3.3e-04 (0.00092)	0.723	1.8e-03 (0.00285)	0.546	-1.7e-06 (0.00175)	0.999	-3.2e-03 (0.00152)	0.055	2.6e-03 (0.00163)	0.112
Snout length	B	B [1:0]	0.78061 (0.00458)	0.03839 (0.00097)	<0.001**	-0.00054 (0.00083)	0.509	-0.00277 (0.00196)	0.157	0.00557 (0.00183)	0.002**	-0.00607 (0.00232)	0.013*	0.00575 (0.00189)	0.002**
Eye vertical position	B	B [0:6]	0.40996 (0.0052)	0.02487 (0.0012)	<0.001**	0.00460 (0.0010)	<0.001**	0.00934 (0.0036)	0.0538	0.00024 (0.0022)	0.912	-0.00031 (0.0024)	0.899	0.00057 (0.0022)	0.794
Head length[3]	B	B [1:7]	2.1453 (0.0232)	0.1347 (0.0034)	<0.001**	0.0074 (0.0025)	0.0034*	-0.0370 (0.0224)	0.162	0.0106 (0.0064)	0.094	-0.0074 (0.0098)	0.455	0.0146 (0.0068)	0.032*
Head width[3]	B	B [8:9]	1.59855 (0.0052)	0.09654 (0.0015)	<0.001**	0.01633 (0.0013)	<0.001**	0.02432 (0.0030)	<0.001**	0.00420 (0.0028)	0.13	-0.00046 (0.0024)	0.85	0.00030 (0.0026)	0.907
Body centroid size	B	From Procrustes analysis	13.1556 (0.0201)	0.9084 (0.0031)	<0.001**	0.0090 (0.0026)	<0.001**	0.0505 (0.0124)	0.0118*	-0.0088 (0.0057)	0.124	0.0253 (0.0099)	0.014*	-0.0227 (0.0061)	<0.001**
Head centroid size	B	From Procrustes analysis	2.2095 (0.0131)	0.1312 (0.0020)	<0.001**	0.0143 (0.0016)	<0.001**	-0.0073 (0.0144)	0.632	0.0077 (0.0037)	0.040*	-0.0075 (0.0050)	0.148	0.0104 (0.0039)	0.008**
Centroid size	Sml	From Procrustes analysis	1.4166 (0.0129)	0.0968 (0.0023)	<0.001**	0.0199 (0.0023)	<0.001**	-0.0387 (0.0102)	0.0111*	0.0033 (0.0042)	0.432	-0.0119 (0.0058)	0.048*	-0.0048 (0.0044)	0.28
Centroid size	Lrg	From Procrustes analysis	3.5944 (0.0177)	0.2598 (0.0029)	<0.001**	0.0601 (0.0029)	<0.001**	0.0202 (0.0133)	0.209	-0.0015 (0.0053)	0.778	-0.0097 (0.0082)	0.244	-0.0054 (0.0056)	0.337

1: The trait values are based on landmarks as numbered and indicated in Supplementary Figure 2.
2: Eye origin is the center point of eye landmarks, and calculated using landmarks 2, 3, 4, and 5, which are the anterior, posterior, dorsal and ventral extremes of the bony orbit of the eye.
3: Landmark 7 is the posterior point of the bony operculum. Landmarks 8 and 9 are the points of maximum curvature of the bony operculum at the ventral and dorsal ends, respectively.

Table 2: Multivariate analysis using Procrustes shape variable across three body planes in juvenile Atlantic salmon. Pillai is the Pillai's trace test statistic to evaluate each term's significance in the multivariate analysis of variance.

Terms	Large cross section				Small cross section				Body			
	df	Pillai	*z* value	*p* value	df	Pillai	*z* value	*p* value	df	Pillai	*z* value	*p* value
Length (scaled)	1	0.207	8.231	0.001	1	0.042	2.574	0.008	1	0.530	15.369	0.001
Condition factor (scaled)	1	0.053	1.398	0.074	1	0.024	0.894	0.195	1	0.478	10.583	0.001
Feed restriction	1	0.096	3.924	0.001	1	0.102	6.035	0.001	1	0.284	12.050	0.001
Family	37	1.939	9.994	0.001	37	0.721	2.200	0.011	37	2.446	24.524	0.001
Tank	4	0.312	6.244	0.001	4	0.219	7.020	0.001	3	0.276	8.643	0.001
Sex	1	0.035	-0.118	0.548	1	0.013	-0.597	0.717	1	0.038	1.185	0.121
vgll3	1	0.042	0.495	0.318	1	0.018	0.108	0.461	1	0.032	0.562	0.285
six6	1	0.027	-0.992	0.831	1	0.013	-0.617	0.739	1	0.052	2.454	0.013
Full model	47	2.727	14.021	0.001	47	1.256	7.674	0.001	46	3.929	23.997	0.001
Residuals	689				681				724			

Table 3: Variance components for 21 morphological traits obtained from three body planes. V_A, h^2, and I_A are additive genetic variance, heritability, and evolvability, respectively, after controlling for length, condition factor, feed restriction, and sex. % $V_{A.vgll3}$ and %$V_{A.six6}$ are additive genetic variation explained by the *vgll3* and *six6* loci, respectively (values are truncated to zero if the estimate is less than zero). Values indicate medians, with 95% CI given in parenthesis.

Trait [1]	Body Plane[2]	V_A	% $V_{A.vgll3}$	%$V_{A.six6}$	h^2	I_A[3]	% rep
Dorsal fin	B	0.0032 (0.0027 - 0.0036)	2.6	0	0.083 (0.072 - 0.095)	0.045 (0.042 - 0.048)	95.2
Anal fin	B	7,7e-04 (6.8 e-04, 8.8e-04)	17.2	0	0.07 (0.061 - 0.08)	0.27 (0.26 - 0.3)	67.3
Pectoral fin	B	0.0027 (0.0024, 0.003)	0	0	0.41 (0.36 - 0.45)	0.016 (0.015 - 0.017)	83.7
Tail fin	B	8.2e-04 (7.3e-04, 9.1e-04)	0	0	0.5 (0.47 - 0.54)	0.051 (0.048 - 0.055)	69.7
Caudal peduncle	B	1e-04 (9.1e-05, 1.2e-04)	0	0	0.26 (0.24 - 0.29)	0.02 (0.019 - 0.021)	65.3
Vertebra thickness	Sml	1.3e-05 (1.1e-05, 1.5e-05)	30.7	0	0.039 (0.033 - 0.045)	0.31 (0.28 - 0.35)	63.7
Vertebra thickness	Lrg	2.0e-05 (1.7e-05, 2.3e-05)	13	0	0.06 (0.052 - 0.069)	0.21 (0.19 - 0.23)	71.4
Cross section diameter	Sml	6.8e-04 (5.9e-04, 7.9e-04)	12.7	0	0.12 (0.11 - 0.14)	0.0099 (0.009 - 0.011)	97.6
Cross section diameter	Lrg	3.3e-04 (2.9e-04, 3.8 e-04)	0	0	0.11 (0.093 - 0.12)	0.012 (0.01 - 0.013)	84.1
Aerobic muscle	Sml	5.8e-05 (5.1e-05, 6.7e-05)	22.4	0	0.19 (0.17 - 0.21)	0.69 (0.62 - 0.76)	56.5
Aerobic muscle	Lrg	7.5e-05 (6.6e-05, 8.7e-05)	0	0	0.37 (0.34 - 0.41)	0.72 (0.65 - 0.79)	24.0
Aerobic muscle vertical extension	Lrg	0.001 (8.6 e-04, 0.0012)	22.2	2.3	0.1 (0.087 - 0.12)	0.29 (0.26 - 0.32)	78.5
Eye diameter	B	3.1e-05 (2.7e-05, 3.5e-05)	8.6	1.6	0.11 (0.094 - 0.12)	0.23 (0.21 - 0.24)	25.9
Snout length	B	9.0e-05 (7.9e-05, 1e-04)	14.1	9.4	0.12 (0.11 - 0.14)	0.023 (0.021 - 0.024)	82.4
Eye vertical position	B	6.4e-05 (5.6e-05, 7.3e-05)	0	0	0.06 (0.052 - 0.069)	0.15 (0.14 - 0.16)	79.7
Head length	B	0.0022 (0.0019, 0.0025)	0	1.8	0.22 (0.19 - 0.26)	0.018 (0.017 - 0.02)	88.9
Head width	B	3.5e-05 (3e-05, 4e-05)	0	0	0.021 (0.018 - 0.025)	0.02 (0.019 - 0.022)	75.4
Body centroid size	B	0.0034 (0.0031, 0.0038)	6.3	4.2	0.47 (0.43 - 0.5)	7.6e-04 (7,1e-04, 8.2e-04)	73.8
Head centroid size	B	5e-04 (4.4e-04, 5.7e-04)	0.5	5.1	0.15 (0.12 - 0.17)	0.009 (0.0084 - 0.0096)	85.1
Centroid size	Sml	8.3e-04 (7.2e-04, 9.5e-04)	4.4	0	0.27 (0.24 - 0.3)	0.043 (0.039 - 0.048)	71.5
Centroid size	Lrg	0.0014 (0.0012, 0.0016)	0	0	0.22 (0.19 - 0.24)	0.0025 (0.0023 - 0.0028)	93.5

1: Trait length unit is cm for all traits.
2: The trait values are based on landmarks as numbered and indicated in Supplementary Figure 2. B, S, and L prefixes represent body, small cross section, and large cross sections, respectively.
3: I_A is measured as V_A divided by the squared trait mean, and it is unit free.

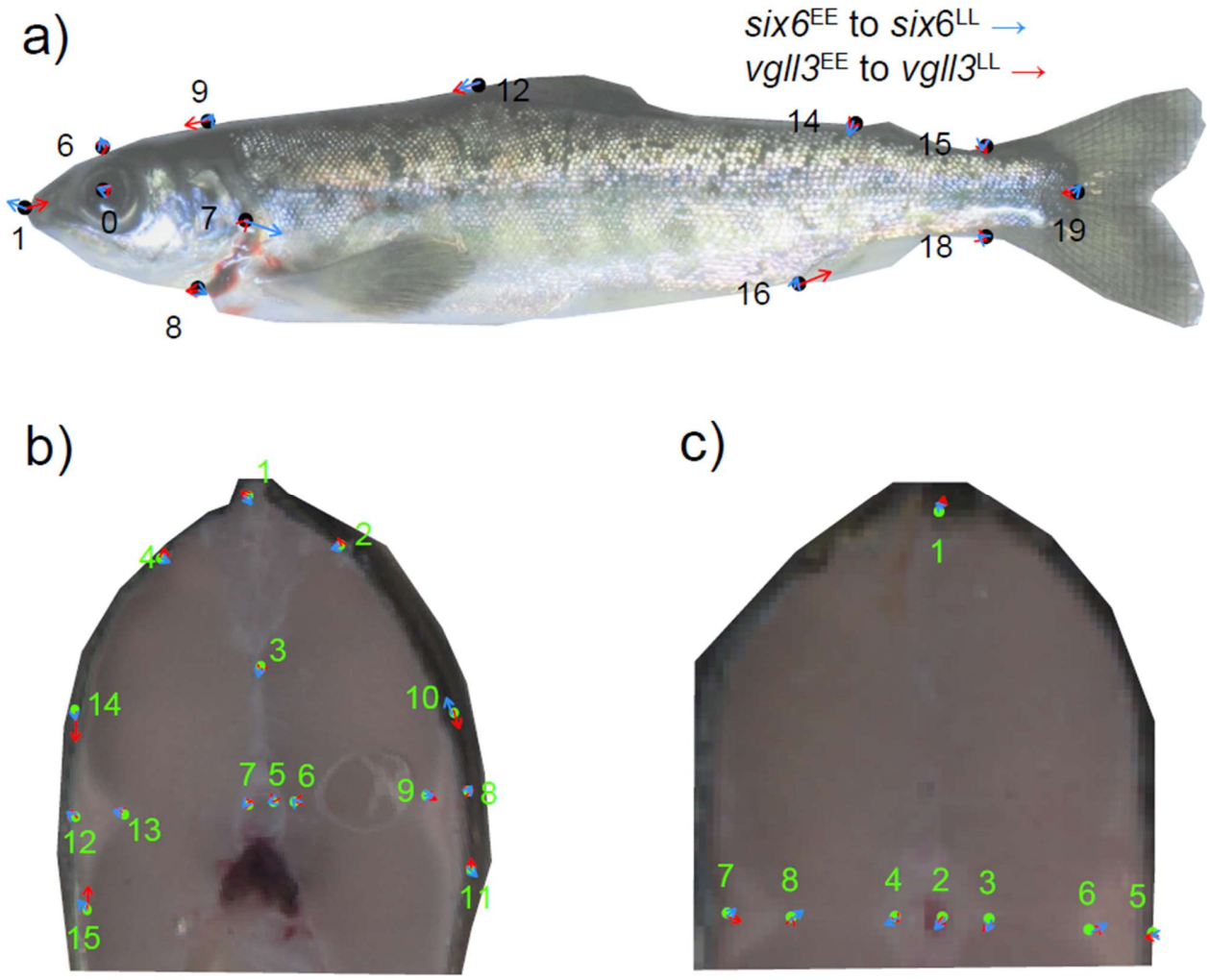

Figure 1: The difference between *vgll3*^{EE} and *vgll3*^{LL} (blue lines), and *six6*^{EE} and *six6*^{LL} (red lines) genotypes on body shape of juvenile Atlantic salmon using thin-plate spline in the body (a), and small (b) and large (b) cross sections. The gray dots are the predicted shape coordinate associated with *vgll3*^{EE} and *six6*^{EE} after the generalized Procrustes analysis. For all images, the effect sizes are magnified by 10x. Landmark numbers are based on Supplementary Figure 2. Note that the body and cross section images are to illustrate the location of landmarks on these body planes, and were slightly distorted to fit onto the average coordinates obtained by Procrustes analysis.

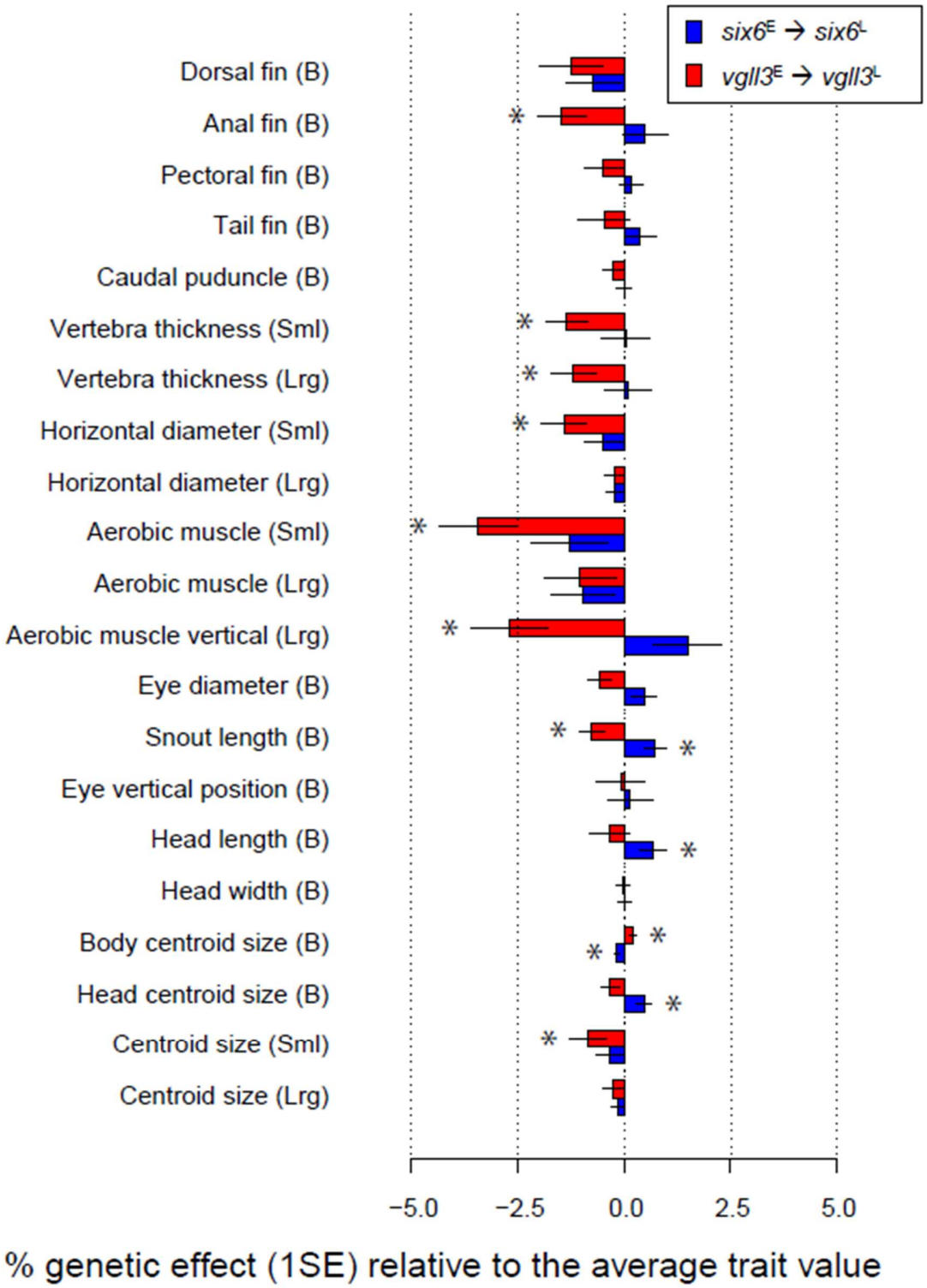

Figure 2: Percent trait value change associated with *vgll3*^{E} to *vgll3*^{L} (red lines), and *six6*^{E} to *six6*^{L} (blue lines) allelic substitutions relative to the average trait values. Asterisks denote significant genetic effect. Error bars and 1SE in the x-axis indicate one standard error.